# Transverse Shear Behavior on the Aeroelastic Stability of Composite Rotor Blades

**Sung Nam Jung* and Seung Jo Kim****

*(Received February 8, 1995)*

The aeroelastic stability of a composite hingeless rotor blade, idealized as a laminated thin-walled box-beam, has been investigated using a finite element formulation based on Hamilton's principle. First-order shear deformation theory and quasi-steady aerodynamic theory have been employed for the analysis. In order to consider the sectional distribution of shear stresses for the box-beam in an effective manner, Timoshenko beam assumption has been made and the formula of shear correction factor of isotropic box section has been used to describe the motion. Three dimensional stress analysis of composite box-beam by using a detailed finite element analysis program has been performed to identify the distribution of shear of the box section and to correlate the results of shear correction factor of isotropic material with that of composite material. Free vibration tests of rotating composite box-beams have showed fairly good agreement between the current results and the experimental data. Transverse shear behavior on the aeroelastic stability has been studied for a specific box-beam configuration. The results displayed in this article have revealed that the transverse shear coupling has a significant role on the flutter boundary of the rotor, especially in case of anti-symmetric configuration.

**Key Words:** Aeroelastic Stability, Thin-Walled Box-Beam, Finite Element Formulation, Shear Correction Factor, Distribution of Shear, Flutter Boundary

## Nomenclature

| | |
|---|---|
| $A$ | : Area of cross-section |
| $C_T$ | : Rotor thrust |
| $c$ | : Blade chord |
| $c_d$ | : Blade section drag coefficient |
| $c_l$ | : Blade section lift coefficient |
| $c_{mac}$ | : Blade section moment coefficient |
| $E_{11}$ | : Young's modulus in fiber direction |
| $E_{22}$ | : Young's modulus in transverse direction |
| $GA$, $SA$, $SP$ | : Sectional moduli |
| $G_{12}$, $G_{13}$ | : Shear moduli |
| $k_{11}$, $k_{22}$ | : Shear correction factors |
| $Q_\eta$, $Q_\zeta$ | : Shear stress resultants |
| $R$ | : Blade length |
| $u$, $v$, $w$ | : Beam deflections |
| $x$, $y$, $z$ | : Undeformed blade coordinates |
| $\alpha$ | : Blade section angle of attack |
| $\varepsilon_{xx}$, $\varepsilon_{x\eta}$, $\varepsilon_{x\zeta}$ | : Engineering strain components |
| $\bar{\theta}$ | : Total geometric pitch of blade( $\bar{\theta} = \theta_0 + \hat{\phi}$) |
| $\theta_0$ | : Blade pretwist angle |
| $\Lambda$ | : Ply orientation angle |
| $\xi$, $\eta$, $\zeta$ | : Deformed blade coordinates |
| $\rho$ | : Mass density |
| $\sigma_{xx}$, $\sigma_{x\eta}$, $\sigma_{x\zeta}$ | : Engineering stress components |
| $\phi$ | : Elastic twist about elastic axis |
| $\hat{\phi}$ | : Geometric twist ( $\hat{\phi} = \phi - \int_0^x \nu_b'' w_b' dx$) |
| $\Omega$ | : Rotor speed |
| $(\ )_h$ | : Horizontal wall of box-beam |
| $(\ )_v$ | : Vertical wall of box-beam |
| $(\ )'$ | : $d/dx$ |

* Department of Aerospace Engineering, Chonbuk National University, Dukjin-Ku, Chonju 560-756, Korea

** Department of Aerospace Engineering, Seoul National University, Kwanak-Ku, Seoul 151-742, Korea

$(\cdot)$ : $d/dt$

## 1. Introduction

The composite materials have been the most popular one in the aerospace applications due to their high-stiffness-to-weight and high-strength-to-weight ratios and superior properties in crashworthiness and damage tolerance over isotropic materials. These superiorities gave the main causes of appearing advanced rotor types such as hingeless and bearingless rotor blades.

In the analysis point of view, the composite rotor blade has typically been analyzed through the one-dimensional beam assumption since the spanwise length of rotor blades is generally much longer than their lateral dimensions. In developing the beam theory, there may be coupling among extension, bending, and torsional deformations. These couplings generally invalidate the Euler-Bernoulli assumption : plane sections remain plane and are perpendicular to the elastic axis. The assumption leads underestimation of beam displacements, especially in case of bending, because of constant shear distribution across the beam section. Moreover, for a composite beam in bending, this distribution of shear is nearly parabolic (piecewise in general) (Whitney, 1973; Vlachoutsis, 1992). The use of shear correction factor (SCF) may be the most economical one to the transverse shear behavior without sacrificing the required accuracy of solution largely. In addition, warping and warping inhibition effects are to be considered in the analysis (Rehfield et. al., 1990). Therefore, an appropriate analytical model capturing these behaviors are inevitable to get more enhanced results of the aeroelastic analysis of a composite rotor blade.

The published works of research on the aeroelastic stability analysis of composite rotor blades were mainly those conducted by Chopra and his associates. Hong and Chopra (1985) used the nonlinear kinematic model of Hodges and Dowell (1974) which was dealt with blades made of isotropic materials, and extended to the case of composite rotor. They used a simplified beam model, in which the transverse shear flexibility was not included in the formulation, but provided a fundamental basis on the flap-lap-torsion aeroelastic analysis of a composite rotor blade. Panda (1987) applied this model to forward flight case and further, Smith and Chopra (1993) modified the previous simple kinematics of beam to include the transverse shear effects and other secondary structural modeling effects. They focused on the behavior of elastically tailored composite blade and presented various results of vibratory hub loads of box-beam having different ply configurations, but they did not go further to consider the sectional distribution of shear stresses. They reported from the structural dynamic analysis of rotating composite beams that the error between the theoretical results and the experimental ones was on the order of 10% (for symmetric lay-up) to 20% (for anti-symmetric lay-up). In order to improve the theoretical results, an alternative approach, which has been developed by Jung and Kim (1994) for the effects of transverse shear and structural damping on the aeroelastic response of composite rotor blades in hover, involved the usage of SCF to account for the sectional distribution of shear stresses. They showed that the effects of transverse shear and structural damping can have a key role on the flutter boundary of the rotor, but the lay-up structure is confined to symmetric configuration only.

In the present work, a finite element approach for the aeroelasic analysis of composite hingeless rotor blade in hovering flight is pursued through a simplified model of laminated thin-walled box-beam. The effects of transverse shear flexibility, torsion warping and two-dimensional inplane behavior are included in the structural formulation. The quasi-steady aerodynamic theory and the perturbation dynamic inflow model of Pitt and Peters (1981) are used in the aerodynamic model. Noncirculatory-origin aerodynamic components are also included. The governing differential equations of motion are obtained by using Hamilton's energy principle. In the finite element model, twenty-three degrees of freedom per element including eight transverse shear degrees of freedom were used to fully consider the flap-lag-

torsion coupled behavior of a composite blade. The use of SCF has been proposed in order to improve the transverse shear behavior of the finite element model. The formula of the SCF of isotropic thin-walled box section by Cowper (1966) was used in the present formulation. Numerical results adressing the effects of transverse shear on the aeroelastic stability are presented for specific box-beam configurations.

## 2. Formulation

The rotor structure is idealized as a laminated composite box-beam whose constituent laminae are characterized by different ply orientation angles and different material and thickness properties (see Fig. 1). The respective four walls of box-beam is assumed to have $N$ layers of homogeneous anisotropic sheets bonded together perfectly. Two Cartesian coordinate systems are used: the $x$-$y$-$z$ undeformed coordinate system and the $\xi$-$\eta$-$\zeta$ deformed coordinate system. The deformation of the blade in space is described by the displacements $u$, $v$, $w$, and $\phi$ which are respectively axial, lead-lag, flap, and elastic twist deformations. The total transverse displacements of in-plane and out-of-plane bending are expressed as the sum of the displacement due to bending and the displacement due to shear deformation.

The strain-displacement relations for small strains and moderately large deformations, up to second order, can be obtained in terms of displacement derivatives in the following form

$$\begin{aligned}
\varepsilon_{xx} &= u' + v_b'^2/2 + w_b'^2/2 - \lambda_T\phi'' + (\eta^2 + \zeta^2)(\theta_0'\phi' + \phi'^2/2) - v_b''(\eta\cos\bar{\theta} - \zeta\sin\bar{\theta}) - w_b''(\eta\sin\bar{\theta} + \zeta\cos\bar{\theta}) \\
\varepsilon_{x\eta}{}^t &= -\left(\zeta + \frac{\partial\lambda_T}{\partial\eta}\right)\phi' \\
\varepsilon_{x\zeta}{}^t &= \left(\eta - \frac{\partial\lambda_T}{\partial\zeta}\right)\phi' \\
\varepsilon_{x\eta}{}^s &= \{v_s'\cos\bar{\theta} + w_s'\sin\bar{\theta}\}f_1(\eta, \zeta) \\
\varepsilon_{x\zeta}{}^s &= \{w_s'\cos\bar{\theta} - v_s'\sin\bar{\theta}\}f_2(\eta, \zeta)
\end{aligned} \tag{1}$$

where subscript $b$ refers to bending deformation and subscript $s$ refers to shear deformation, $\lambda_T$ is the torsion-related warping function (Smith et al., 1991), and $f_1$, $f_2$ are arbitrary functions of sectional coordinates $\eta$ and $\zeta$. The functions, $f_1$ and $f_2$, are to be modified in suitable forms to perform the analysis of composite beam effectively by imposing an assumption like Timoshenko beam assumption (1921), because the distribution of shear of the beam section has nearly parabolic. In this formulation, first-order shear deformation theory was adopted to treat this kind of problem. In the above equation, based on the superposition principle, shear strain components, $\varepsilon_{ij}$, are decomposed into torsion-related engineering strain components, $\varepsilon_{ij}{}^t$, and transverse-shear-related engineering strain components, $\varepsilon_{ij}{}^s$.

The constitutive relations of horizontal and vertical laminae of box-beam walls have the following form

$$\begin{Bmatrix}\sigma_{xx}\\ \sigma_{x\eta}\end{Bmatrix} = \begin{bmatrix}\bar{Q}_{11} & \bar{Q}_{16}\\ \bar{Q}_{16} & \bar{Q}_{66}\end{bmatrix}\begin{Bmatrix}\varepsilon_{xx}\\ \varepsilon_{x\eta}\end{Bmatrix}$$
$$\begin{Bmatrix}\sigma_{xx}\\ \sigma_{x\zeta}\end{Bmatrix} = \begin{bmatrix}\bar{Q}_{11} & \bar{Q}_{16}\\ \bar{Q}_{16} & \bar{Q}_{66}\end{bmatrix}\begin{Bmatrix}\varepsilon_{xx}\\ \varepsilon_{x\zeta}\end{Bmatrix} \tag{2}$$

where the expressions for the etransformed reduced stiffness matrix $\bar{Q}_{ij}$ in terms of material constants are given in Jones (1975). In case of thin-walled construction of box-beam, the internal shear stresses for the equivalent load applying at shear center are distributed in a form as shown in Fig. 2. Since the distribution of shear strain (or stress) in the load direction of the wall is shown to have nearly parabolic function (see Fig. 3), an appropriate treatment of the distribution of shear is required to the one-dimensional beam kinematics. Based on the equivalent energy con-

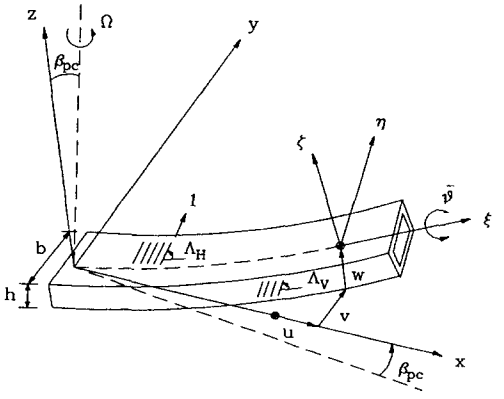


**Fig. 1** Composite box beam geometry and deflections

cept, the shear correction factors are introduced in the present beam formulation to describe the shear motion. Accordingly, the aforementioned functions $f_1$ and $f_2$, which are corresponds to SCFs after all, have constant values. The equilibrium relations for the box-beam composed of orthotropic laminates can be written in the form

$$\begin{Bmatrix} Q_\eta \\ Q_\zeta \end{Bmatrix} = \begin{bmatrix} k_{11}GA_h & 0 \\ 0 & k_{22}GA_v \end{bmatrix} \begin{Bmatrix} v_s' \cos\bar{\theta} + w_s' \sin\bar{\theta} \\ w_s' \cos\bar{\theta} - v_s' \sin\bar{\theta} \end{Bmatrix} \tag{3}$$

where $Q_\eta$ and $Q_\zeta$ are shear stress resultants in horizontal and vertical directions of box-beam, $GA_h$ and $GA_v$ are the respective shear moduli, and $k_{11}$ and $k_{22}$ are the SCFs for in-plane and out-of-plane directions, respectively.

The variation of strain energy for the composite blade can be written by

$$\delta U = \int_0^R \iint_A (\sigma_{xx}\delta\varepsilon_{xx} + \sigma_{x\eta}\delta\varepsilon_{x\eta} + \sigma_{x\zeta}\delta\varepsilon_{x\zeta}) d\eta d\zeta dx \tag{4}$$

Substituting the stress-strain and strain-displacement relations into the above equation of strain energy, and taking Eq. (3) into account, we obtain the variational form of the strain energy in terms of displacement components. In obtaining the expression of strain energy variation, an ordering scheme similar to Hodges, et. al.(1974) is used to systematically eliminate higher order nonlinear terms. It is assumed that transverse shear deformations, $v_s$ and $w_s$ are of order $\varepsilon^{3/2}$ compared to bending deformations, $v_b$ and $w_b$, of order $\varepsilon$, and the other field variables have the same order of magnitudes as described in Hodges, et. al.(1974) The resulting strain energy expression is consisted of so many terms of displacement derivatives and may be written symbolically in a convenient manner as

$$\delta U = \delta U_{iso} + \delta U^0{}_{comp} + \delta U^s{}_{comp} \tag{5}$$

where the first term of right hand side of the euqation $\delta U_{iso}$ represents the strain energy components of an isotropic blade (truly the same form, but the sectional constants are modified to have the information of anisotropic characteristics of composite laminates), and the rest two terms represent the additional strain energy components due to the elastic coupling effects of composite blade: $\delta U^0{}_{comp}$ is the usual component of strain energy which does not include the transverse shear deformations, and $\delta U^s{}_{comp}$ is the transverse-shear-related component of strain

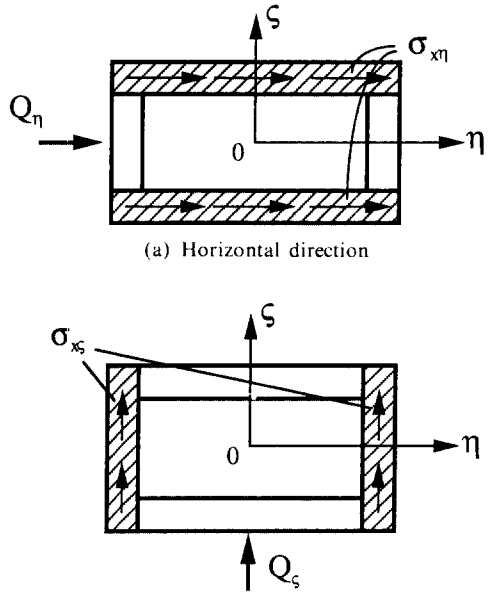


**Fig. 2** The distribution of shear stresses due to applied forces

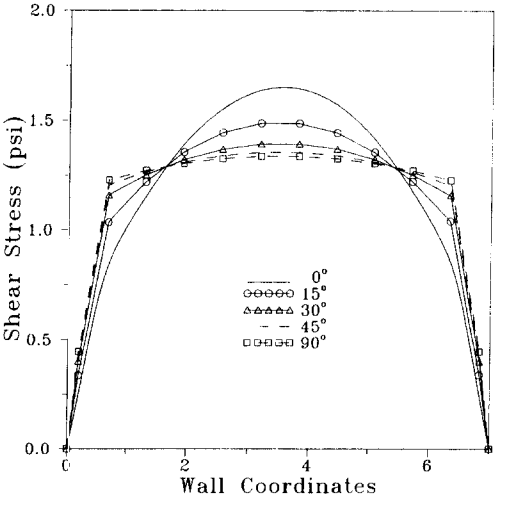


**Fig. 3** The distribution of shear stresses in the horizontal wall of box beam with ply angle changes

energy. The expression of the strain energy variation of $\delta U_{iso}$ and $\delta U^0{}_{comp}$ can be found in Hong, et. al.(1985), and the additional component $\delta U^s{}_{comp}$ is developed as follows

$$\begin{aligned}\delta U^s{}_{comp}=\int_0^R [&k_{11}GA_h\{(v_s'\cos^2\theta_0+w_s'\sin\theta_0\cos\theta_0)\delta v_s'\\&+(v_s'\sin\theta_0\cos\theta_0+w_s'\sin^2\theta_0)\delta w_s'\}+k_{22}GA_v\{(v_s'\sin^2\theta_0-w_s'\sin\theta_0\cos\theta_0)\delta v_s'\\&-(v_s'\sin\theta_0\cos\theta_0-w_s'\cos^2\theta_0)\delta w_s'\}+k_{13}SP_h\{(v_b''\sin\theta_0\cos\theta_0-w_b''\cos^2\theta_0)\delta v_s'\\&+(v_b''\sin^2\theta_0-w_b''\sin\theta_0\cos\theta_0)\delta w_s'\}+k_{23}SP_v\{(v_b''\sin\theta_0\cos\theta_0+w_b''\sin^2\theta_0)\delta v_s'\\&-(v_b''\cos^2\theta_0+w_b''\sin\theta_0\cos\theta_0)\delta w_s'\}+k_{13}SP_h\{(v_s'\sin\theta_0\cos\theta_0+w_s'\sin^2\theta_0)\,\delta v_b''\\&-(v_s'\cos^2\theta_0+w_s'\sin\theta_0\cos\theta_0)\delta w_b''\}+k_{23}SP_v\{(v_s'\sin\theta_0\cos\theta_0-w_s'\cos^2\theta_0)\delta v_b''\\&+(v_s'\sin^2\theta_0-w_s'\sin\theta_0\cos\theta_0)\delta w_b''\}\\&+k_{13}SA_h(u'+v_b'^2/2+w_b'^2/2)(\cos\theta_0\delta v_s'+\sin\theta_0\delta w_s')\\&+k_{23}SA_v(u'+v_b'^2/2+w_b'^2/2)(\cos\theta_0\delta w_s'-\sin\theta_0\delta v_s')\\&+k_{13}SA_h(v_s'\cos\theta_0+w_s'\sin\theta_0)(\delta u'+v_b'\delta v_b'+w_b'\delta w_b')\\&+k_{23}SA_v(w_s'\cos\theta_0-v_s'\sin\theta_0)(\delta u'+v_b'\delta v_b'+w_b'\delta w_b')]\,dx\end{aligned}\tag{6}$$

where $k_{13}$ and $k_{23}$ are the shear correction factors for bending-shear coupling, which are introduced to keep the consistency of describing the strain energy expression, and used "1" unless otherwise specified. The sectional coefficients $GA_i$, $SA_i$, and $SP_i$ $(i=h$ or $v)$ are shear modulus, extension-shear coupling modulus of symmetric configurations, and bending-shear coupling modulus of anti-symmetric configurations, respectively. The coefficients appeared in Eq. (6) are defined as follows.

$$\begin{aligned}GA_h&=\iint_{A_h} C_{66}d\eta d\zeta\\GA_v&=\iint_{A_v} C_{66}d\eta d\zeta\\SA_h&=\iint_{A_h} C_{16}d\eta d\zeta\\SA_v&=\iint_{A_v} C_{16}d\eta d\zeta\\SP_h&=\iint_{A_h} C_{16}\zeta d\eta d\zeta\\SP_v&=\iint_{A_v} C_{16}\eta d\eta d\zeta\end{aligned}\tag{6a}$$

where $C_{ij}$'s are the modified inplane stiffnesses based on the plane stress condition to address the transverse inplane behavior of composite laminates (Smith et. al., 1991).

The kinetic energy for a composite blade can be expressed as the same form for a metal blade except the additional components of kinetic energy due to the incorporation of transverse shear deformations. The complete details of the kinetic energy expression can be found in Jung, et. al.(1994). While the total displacement of the blade is expressed as the sum of the displacement due to bending and shear, the aerodynamic loads induced by the blade motion is also the sum of the loads due to bending and shear deformation. The circulatory aerodynamic forces are obtained from the quasi-steady strip theory, and the virtual work done by the nonconservative aerodynamic forces has the form.

$$\begin{aligned}\delta W_e=\int_0^R &\{L_u\delta u+(L_{v_b}+L_{v_s})(\delta v_b+\delta v_s)\\&+(L_{w_b}+L_{w_s})(\delta w_b+\delta w_s)+M_\phi\delta p\}dx\end{aligned}\tag{7}$$

where $L_u$ and $M_\phi$ are the aerodynamic force and moment distributed along the length of the blade in axial and twist directions, $L_{v_b}$ and $L_{v_s}$ denote the edgewise components of aerodynamic forces in bending and shear parts, and $L_{w_b}$ and $L_{w_s}$ denote the flapwise components of aerodynamic loads in bending and shear deformations, respectively. The $\delta$p is the virtual rotation of a point on the deformed elastic axis of the beam. The noncirculatory-origin aerodynamic components are also included in this variational equation.

The governing differential equations of motion are obtained by using the extended Hamilton principle. The discretized form in the finite elements can be written by

$$\int_{t_1}^{t_2}\sum_{i=1}^{Ne}(\delta U_i-\delta T_i-\delta W_{ei})dt=0\tag{8}$$

where $N_e$ is the total number of finite elements, and the subscript $i$ denotes the contribution of an i-th element. Each beam element consists of two end nodes and three internal nodes, which results in a total of 23 degrees of freedom (DOF) element including eight transverse shear degrees of freedom. The element has 10 DOF at each of the two end nodes: the deflections due to bending, $v_b$ and $w_b$, the deflections due to shear, $v_s$ and $w_s$, and their derivatives with respect to $x$, the axial displacement $u$, and the twist angle $\phi$. Among the three internal nodes, two are for $u$ and one for $\phi$. The final nonlinear equations of motion in terms of nodal degrees of freedom $q$ are obtained by using the above Eq. (8), which result in

$$\boldsymbol{M}(\boldsymbol{q})\ddot{\boldsymbol{q}}+\boldsymbol{C}(\boldsymbol{q})\dot{\boldsymbol{q}}+\boldsymbol{K}(\boldsymbol{q})\boldsymbol{q}=\boldsymbol{F} \tag{9}$$

where $\boldsymbol{M}$, $\boldsymbol{C}$, $\boldsymbol{K}$, and $\boldsymbol{F}$ are the global inertia, damping, stiffness matrices and load vector, respectively.

## 3. Solution Procedures

The first step in solving the Eq. (9) is to get the steady equilibrium position. The blade steady-state equations are obtained by neglecting all time dependent terms in the equation of motion. The nonlinear trimmed states of the blade are calculated iteratively by using the standard Newton-Raphson technique, which generally guarantees quadratic convergence, and several iteration steps are performed to insure the accuracy of the solutions. In the next stage, the free vibration analysis of the rotating blade about the equilibrium position is carried out to determine the natural modes of the blade. A modal coordinate transformation based on these normal modes is then performed to reconstruct the system inertia, damping, and stiffness matrices. A dynamic inflow model of Pitt and Peters (1981) is used to consider the unsteady aerodynamic effects at the following stage of flutter analysis. In a final stage, the stability analysis of the blade is conducted from the modal flutter equation, which is to be transformed to first order system and solved as an algebraic eigenvalue problem.

## 4. Results and Discussion

The SCF of isotropic thin-walled box section can be determined analytically by beam flexure problem and is function of sectional coordinates and Poisson ratio, like the form given by Cowper (1966). However, in composite box-beam analysis, the problem requires additional considerations, such as lamination configuration and flexure-torsion coupled behavior owing to the existence of elastic couplings inherent in composite laminates. Much work is required to the exact evaluation of SCF for the composite box-beam, as inferred from the work of Kosmatka (1993) for the behavior of a tip-loaded cantilever beam with an arbitrary cross section. Instead of obtaining the SCF of composite box-beam, the equation of SCF driven by Cowper which was verified in Jung, et. al.(1994) was used in the present work, and the distribution of shear was identified with a three-dimensional stress analysis by the MSC/NASTRAN. The analysis model has 2624 node points and 1280 HEXA eight-node brick elements, which use bubble function to prevent shear locking. The ply angle of the box-beam has the same orientation in a global sense, mainly for the restriction of size in the finite element model. When a load is applied at beam tip, the internal stresses are induced to satisfy the force equilibrium. Figure 3 shows the distribution of shear obtained from the Gauss points located at the center of the cubic element in the horizontal wall of box-beam with respect to layer angle changes. A parabolic type of distribution of shear stress, except the corner area of box section showing some kind of discontinuities, is obtained as seen in the plot. This discontinuity is due in part to the finite element mesh used in the present beam model, and more fine meshes are needed to remedy this kind of problem. In that case, however, computing time is more heavier than the present one owing to the increase of problem size. The other causes of discontinuity is the existence of elastic couplings and geometric peculiarities of composite box-beam. The figure shows that the irregular region is confined to the local area

(intersected area of horizontal and vertical wall of box section), and the other parts occupying almost all of the wall has parabolic distribution as expected. It is noted in the plot that, as the ply angle varied from 0° to 90°, the peak value of stress is going down, i.e., it gets flattens. This fact may give one the idea that the effects of shear correction are also lessens with the increase of ply angles.

Figure 4 presents the influence of rotational speed on the first three lowest frequencies (first two flap and first lag) of a graphite-epoxy box beam with $[30]_6$ in top and $[30/\text{-}30]_3$ in side walls, which induces bending-torsion coupling of the beam. The mechanical properties were used as (Smith et. al., 1993) : $E_{11}=141.9$ GPa, $E_{22}=9.790$ GPa, $G_{12}=G_{13}=6.134$ GPa, $\nu_{12}=0.42$, and $\rho=1$, 445 kg/m$^3$. The calculated SCFs in this model were $k_{11}=0.6030$ and $k_{22}=0.2773$. The present results of the figure are expressed as lines and the experimental results (Chandra et. al., 1992) are denoted as circles. The experimental data were obtained in a vacuum test facility for the better understanding of the structural couplings of composite rotors without the effects of nonconservative aerodynamic forces. A good correlation between theoretical and experimental results is clearly seen in the plot. Figure 5 shows similar results for $[45]_6$ graphite-epoxy beams. The deviation of the two results is larger than the previous $[30]_6$ box beam, but the correlation is generally within 10%. The increase of the fundamental frequency (1st flap) due to the inclusion of rotating effect is 54.2%.

Nextly, numerical simulations are conducted to see the effects of transverse shear deformations on the aeroelastic behavior of composite rotor. The results are obtained for a hingeless rotor blade with Lock number $\gamma=5.0$, solidity ratio $\sigma=0.1$, chord to span ratio $c/R=0.08$, and zero precone. The chordwise offsets of the center of mass, aerodynamic center, and tension center from the elastic axis are assumed to be zero. The airfoil characteristics used were : $c_l=5.7\,\alpha$, $c_d=0.01$, and $c_{mac}=0$. The blade structure is represented by a laminated composite box-beam composed of four walls. Five normal modes (two flap, two lag, and one torsion) calculated at the deformed equilibrium position of the blade are used to perform the stability analysis. A baseline balde configuration has stiff-inplane property as : the first flap frequency $\omega_w=1.15$/rev, the first lag frequency $\omega_v=1.5$/rev, and the first torsion frequency $\omega_\phi=5.0$. Stability results are obtained for symmetric (CASE I) and anti-symmetric (CASE II) configurations (see Fig. 6). In a symmetric configuration,

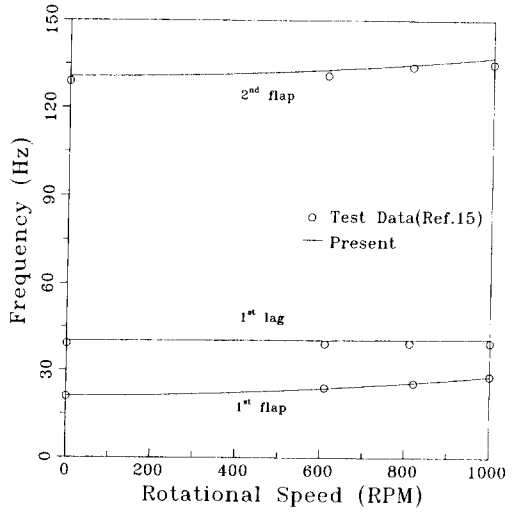


**Fig. 4** Comparison of natural frequencies of $[30]_6$ box beam at various rotational speeds

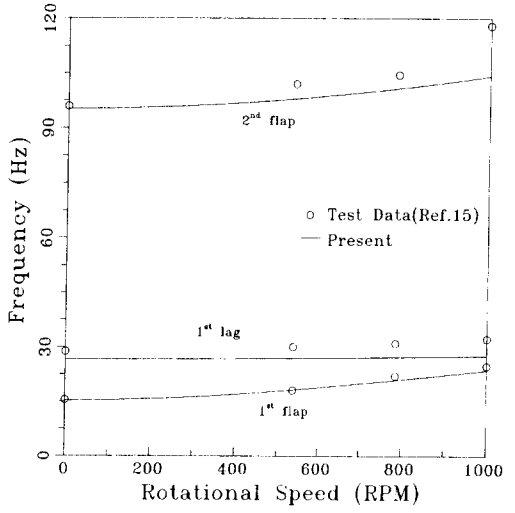


**Fig. 5** Comparison of natural frequencies of $[45]_6$ box beam at various rotational speeds

the ply lay-ups on opposite walls with respect to geometric center of box section are identical while, for an anti-symmetric configuration, the ply lay-ups on opposite walls are of reversed orientation. However, each of the four laminates has symmetric lay-ups about the respective middle surfaces as shown in Fig. 6. The length, $R$, of the rotor is 4.42m and the cross-section of the beam has an outside dimension of 0.178m width by 0.051m height with $8.89\times10^{-3}$m thick. The mechanical properties of composites used herein were: $E_{11}=206.7$ GPa, $E_{22}=20.67$ GPa, $G_{12}=G_{13}=8.270$ GPa, $\nu_{12}=0.3$, and $\rho=1{,}742\text{kg/m}^3$. The calculated SCFs in this model were $k_{11}=0.7377$ and $k_{22}=0.1264$.

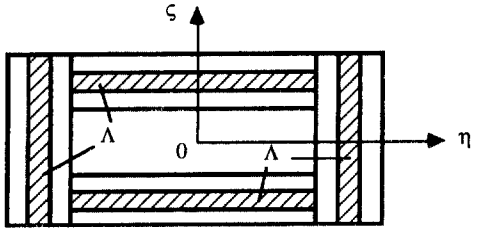


(a) Symmetric layup(CASE I)

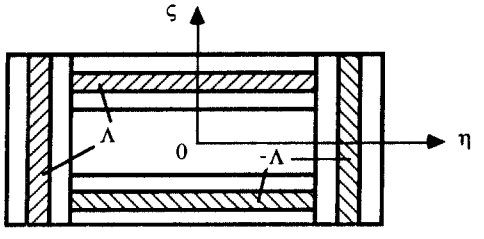


(b) Anti-symmetric layup (CASE II)

**Fig. 6** Lay-up geometry of CASE I and CASE II

Figures 7 and 8 show the root locus plots of complex eigenvalues as a function of fiber angle $\Lambda$ for the first lag and flap modes, respectively, at a thrust level of $C_T/\sigma=0.1$ (CASE I), as the layer angles vary from 0 to 180 deg. The figures show that the ply angle change has a considerable influence on the stability roots of the blade. It is shown that the effects of transverse shear on the stability solution for these modes having symmetric configuration are not large. With the inclusion of transverse shear, there is a slight decrease in frequency and generally a small reduction in damping of the modes. In other words, the transverse shear flexibility softens the modes and destablizes the motions slightly.

Figures 9 and 10 show the root locus plots of CASE ‖ configuration with changing ply angle $\Lambda$ for the first lag and flap modes, respectively, at a thrust level of $C_T/\sigma=0.1$. For this configuration, the major coupling terms affecting the composites behavior are bending-shear and extension-torsion couplings. The stability roots of the blade having anti-symmetric lay-ups are shown to be largely changed by this coupling terms. The effect

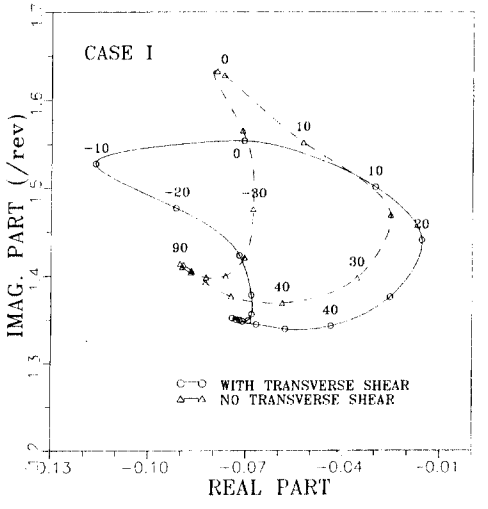


**Fig. 7** Transverse shear effects on the first lag mode in symmetric configurations

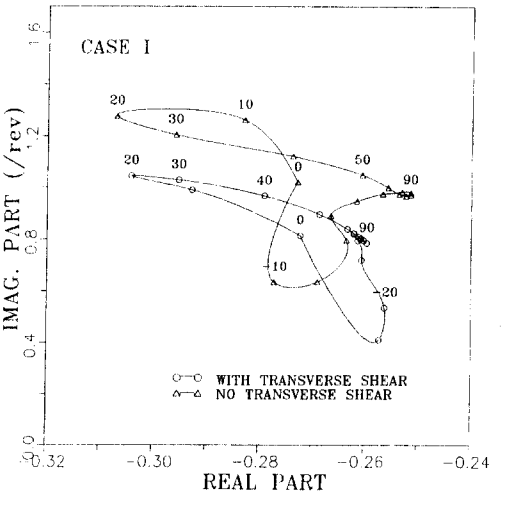


**Fig. 8** Transverse shear effects on the first flap mode in symmetric configurations

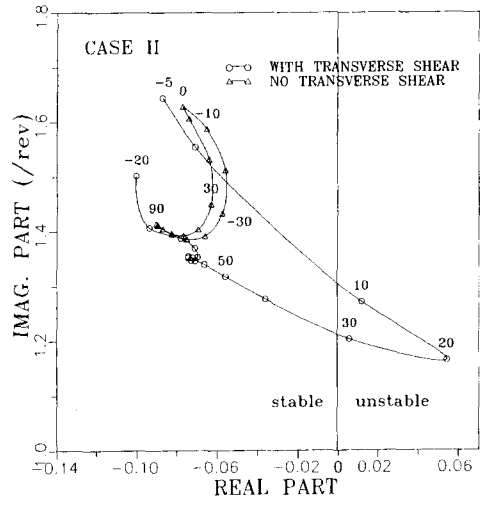


**Fig. 9** Transverse shear effects on the first lag mode in antisymmetric configurations

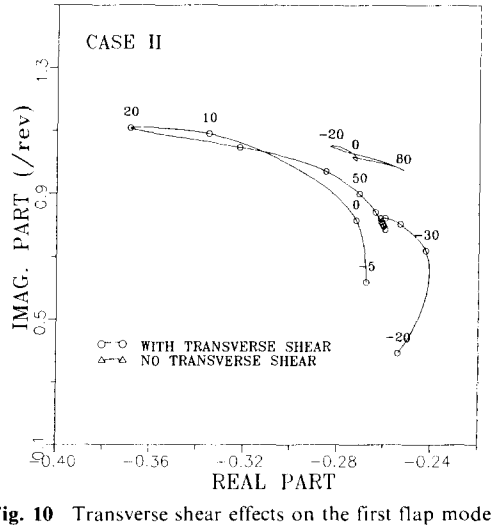


**Fig. 10** Transverse shear effects on the first flap mode in antisymmetric configurations

of transverse shear on the lag mode eigenvalues is quite large on the damping of the mode as seen in Fig. 9. With the inclusion of transverse shear, the instability occurs at layer angles of 10 to 30 deg. In general, the transverse shear tends to lower the frequency of the mode and destabilizes the motion largely, but the effect is reversed at $\Lambda$ of-10 to-30 deg. This fact is closely related with the following results of Fig. 10. Figure 10 depicts that the transverse shear effect on the flap mode frequency is quite significant. Positive $\Lambda$ stiffens the flap mode and negative $\Lambda$ softens this one. Very low flap frequency of the blade is obtained for $\Lambda$ of-10 to-20 deg. The blade seems to be placed in a statically unstable state (torsional divergence) at these ply angles. This critical condition thought to be brought out the unusual results of lag mode eigenvalues at layer angles of-10 to-30 deg.

## 5. Conclusion

A finite element formulation of aeroelastic equations for the analysis of composite helicopter rotor blades in hover has been presented. The effects of transverse shear deformation was incorporated in the formulation. A three-dimensional stress analysis for a composite box-beam model has been conducted to identify the distribution of shear in the box-beam wall by a detailed finite element analysis program. The analysis has revealed that the distribution of shear has near parabolic shape in spite of ply angle changes. The shear correction factors have been introduced to account for this sectional distribution of shear effectively. The present results of the rotating composite box beams turns out to have good correlation with experimental data. The aeroelastic analysis of composite rotor having symmetric and anti-symmetric configuration has also been carried out. The effects of transverse shear on the aeroelastic behavior of the rotor were seen to be very important, especially in case of anti-symmetric configuration. In this type of configuration, the inclusion of shear affects the system on both the frequency and the damping in a very large scale. It is recommended from the analysis that the transverse shear flexibility considering the distribution of shear should be kept for the analysis of composite rotor to get more enhanced results.

## Acknowledgements

This work was partially supported by Chonbuk National University. This support is gratefully acknowledged.

## References

Chandra, R. and Chopra, I., 1992, "Expe-

rimental-Theoretical Investigation of the Vibration Characteristics of Rotating Composite Box Beams," *Journal of Aircraft*, Vol. 29, No. 4, pp. 657~664.

Cowper, G. R., 1966, "The Shear Coefficient in Timoshenko's Beam Theory," *Journal of Applied Mechanics*, pp. 335~340.

Hodges, D. H. and Dowell, E. H., 1974, "Nonlinear Equations of Motion for the Elastic Bending and Torsion of Twisted Nonuniform Blades," NASA TN D-7818.

Hong, C. H. and Chopra, I., 1985, "Aeroelastic Stability Analysis of a Composite Rotor Blade," *Journal of the American Helicopter Society*, Vol. 30, No. 2, pp. 57~67.

Jones, R. M., 1975, *Mechanics of Composite Materials*, McGraw-Hill, New York.

Jung, S. N. and Kim, S. J., 1994, "Aeroelastic Response of Composite Rotor Blades Considering Transverse Shear and Structural Damping," *AIAA Journal*, Vol. 32, No. 4, pp. 820~827.

Kosmatka, J. B., 1993, "Flexure-Torsion Behavior of Prismatic Beams, Part I : Section Properties via Power Series," *AIAA Journal*, Vol. 31, No. 1, pp. 170~179.

Panda, B. and Chopra I., 1987, "Dynamics of Composite Rotor Blades in Forward Flight," *Vertica*, Vol. 11, No. 1/2, pp. 107~209.

Pitt, D. M. and Peters, D. A., 1981, "Theoretical Prediction of Dynamic Inflow Derivatives," *Vertica*, Vol. 5, No. 1, pp. 21~34.

Rehfield, L. W., Atilgan, A. R. and Hodges, D. H., 1990, "Nonclassical Behavior of Thin-Walled Composite Beams with Closed Cross Section," *Journal of the American Helicopter Society*, Vol. 35, No. 2, pp. 42~50.

Smith, E. C. and Chopra, I., 1991, "Formulation and Evaluation of an Analytical Model for Composite Box-Beams," *Journal of the American Helicopter Society*, Vol. 36, No. 3, pp. 23~25.

Smith, E. C. and Chopra, I., 1993, "Aeroelastic Response, Loads and Stability of a Composite Rotor in Forward Flight," *AIAA Journal*, Vol. 31, No. 7.

Timoshenko, S. P., 1921, "On the Correction for Shear of the Differential Equations for Transverse Vibrations of Prismatic Beams," *Philosophical Magazine*, Vol. 41, No. 8, pp. 744~746.

Vlachoutsis, S., 1992, "Shear Correction Factors for Plates and Shells", *International Journal for Numerical Methods in Engineering*, Vol. 33, pp. 1537~1552.

Whitney, J., M., 1973, "Shear Correction Factors for Orthotropic Laminates Under Static Load," *Journal of Applied Mechanics*, Vol. 40, pp. 302~304.